



A Journal of the Gesellschaft Deutscher Chemiker

Angewandte Chemie

GDCh

International Edition

www.angewandte.org

Accepted Article

Title: New series of MAX phases with MA-triangular-prism bilayers: synthesis, structure, and elastic properties

Authors: Hongxiang Chen, Dongliang Yang, Qinghua Zhang, Shifeng Jin, Liwei Guo, Jun Deng, Xiaodong Li, and Xiaolong Chen

This manuscript has been accepted after peer review and appears as an Accepted Article online prior to editing, proofing, and formal publication of the final Version of Record (VoR). This work is currently citable by using the Digital Object Identifier (DOI) given below. The VoR will be published online in Early View as soon as possible and may be different to this Accepted Article as a result of editing. Readers should obtain the VoR from the journal website shown below when it is published to ensure accuracy of information. The authors are responsible for the content of this Accepted Article.

To be cited as: *Angew. Chem. Int. Ed.* 10.1002/anie.201814128
Angew. Chem. 10.1002/ange.201814128

Link to VoR: <http://dx.doi.org/10.1002/anie.201814128>
<http://dx.doi.org/10.1002/ange.201814128>

COMMUNICATION

New series of MAX phases with MA-triangular-prism bilayers: synthesis, structure, and elastic properties

Hongxiang Chen, Dongliang Yang, Qinghua Zhang, Shifeng Jin, Liwei Guo, Jun Deng, Xiaodong Li, Xiaolong Chen*

Abstract: We report a new type of MAX phase, $\text{Nb}_3\text{As}_2\text{C}$, designated as 321 phase. It differs from all the known $\text{M}_{n+1}\text{AX}_n$ phases in that it consists of an alternate stacking of one MX layer and two MA layers in its unit cell, while only one MA layer is allowed in usual MAX phases. The new 321 phase exhibits a bulk modulus of $\text{Nb}_3\text{As}_2\text{C}$ up to 225(3) GPa as determined by high pressure synchrotron X-ray diffraction, one of the highest values among the known MAX phases. Isostructural 321 phases $\text{V}_3\text{As}_2\text{C}$, $\text{Nb}_3\text{P}_2\text{C}$ and $\text{Ta}_3\text{P}_2\text{C}$ are also found to exist. First-principles calculations reveal the outstanding elastic stiffness in 321 phases. Among all 321 phases, $\text{Nb}_3\text{P}_2\text{C}$ is predicted to possess the highest elastic properties. These 321 phases, represented by a chemical formula $\text{M}_{n+1}\text{A}_n\text{X}$, were added as new members to the MAX family and their other properties deserve future investigations.

MAX phases^[1] belong to a family of non-van-der-Waals-type layered compounds with a general formula of $\text{M}_{n+1}\text{AX}_n$ ($n = 1, 2, 3$) in which M = transition metals, A = main group elements, and X = C/N. MAX phases are also termed as metallic ceramics^[2] for their combined characteristic properties of both ceramics and metals. Some of them host high thermal and electrical conductivity, good elastic performance, excellent resistance to corrosion, oxidation, and thermal shock, easy machinability and unusual damage-tolerance^[2a, 3]. These combined elastic,

electrical and thermal properties enable them to be promising materials for various applications^[4], especially in the structural or conductive components under high temperatures. Besides, MAX phases also have drawn much attention as the precursor of MXenes^[5]. Owing to the relatively weak bonding of M-A in MAX phases, a series of two dimensional transition metal carbides can be obtained from acid etching of selected MAX phases^[6].

The study of MAX phases started from 1960s when the H-phases were found by Nowotny's group^[7]. Now, over 60 MAX phases are found. Depending on the value of n , the M_2AX , M_3AX_2 and M_4AX_3 phases are usually named as 211, 312 and 413 phases, respectively^[1b]. The crystal structures of MAX phases usually share a common symmetry with space group $P6_3/mmc$. Each X atom is coordinated by six M atoms forming an octahedron, and each M atom by six A atoms forming a hexagonal prism as shown in Figure 1. $\text{M}_{n+1}\text{AX}_n$ can be regarded as an alternate stacking of n MX layers consisting of the edge-shared M_6X octahedrons and one MA layer consisting of edge-shared M_6A triangular prisms. It should be noted that two and three MX layers can be combined into edge-shared bilayer and trilayer as in 312^[8] and 413^[9] phases, respectively. Besides, $\text{Mo}_2\text{Ga}_2\text{C}$ ^[10], $\text{Ta}_2\text{S}_2\text{C}$, $\text{Ta}_2\text{Se}_2\text{C}$ ^[11], and $\text{Nb}_2\text{S}_2\text{C}$ ^[12], named as 221 phases, also have a similar structure with $\text{M}_{n+1}\text{AX}_n$ phases, where two layers of A atoms exist between the MX layers. The multi-layering of MA layers, however, has never been found among the known MAX phases.

[*] Dr. H. Chen, Dr. Q. Zhang, Dr. S. Jin, J. Deng, Prof. Dr. L. Guo, Prof. Dr. X. Chen
Research & Development Center for Functional Crystals, Laboratory of Advanced Materials and Electron Microscopy
Beijing National Laboratory for Condensed Matter Physics, Institute of Physics, Chinese Academy of Sciences
Beijing 100190, China
E-mail: chenx29@iphy.ac.cn
Dr. H. Chen
School of Materials Science and engineering
Fujian University of Technology
Fuzhou 350118, China
Dr. D. Yang, and Prof. Dr. X. Li
Beijing Synchrotron Radiation Facility
Institute of High Energy Physics, Chinese Academy of Science, Beijing 100049, China
J. Deng, Prof. Dr. X. Chen
School of Physical Sciences
University of Chinese Academy of Sciences
Beijing 101408, China
Prof. Dr. X. Chen
Collaborative Innovation Center of Quantum Matter
Beijing 100084, China
Prof. Dr. L. Guo
Center of Materials Science and Optoelectronics Engineering
University of Chinese Academy of Sciences
Beijing 100049, China
Prof. Dr. L. Guo
Songshan Lake Materials Laboratory
Dongguan, Guangdong 523808, China

Supporting information for this article is given via a link at the end of the document.

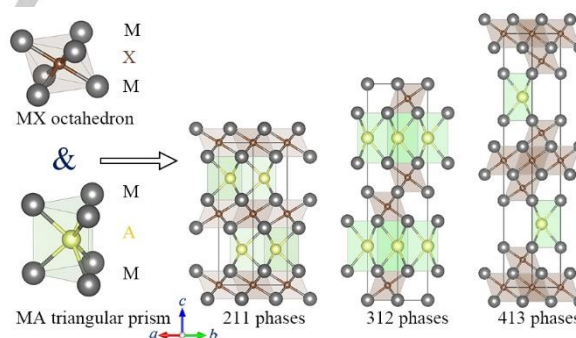


Figure 1. The crystal structure of $\text{M}_{n+1}\text{AX}_n$ phases. The schematic of the M_6X octahedron and M_6A triangular prism in MAX phases, and the crystal structure of 211, 312, and 413 phases viewed from [110] direction.

In this Communication, we report new MAX phases in As-, P-contained systems, namely, $\text{Nb}_3\text{As}_2\text{C}$, $\text{V}_3\text{As}_2\text{C}$, $\text{Nb}_3\text{P}_2\text{C}$, and $\text{Ta}_3\text{P}_2\text{C}$. Their crystal structures are determined by X-ray diffraction (XRD) and high resolution transmission electron microscopy (HRTEM). These isostructural phases can be regarded as formation from the alternate stacking of one MX layer and two MA layers in their unit cell. They can be expressed as $\text{M}_{n+1}\text{A}_n\text{X}$ ($n=2$), henceforth referred to as 321 phases. In contrast to the known MAX phases, here the multi-layered MA layer is

COMMUNICATION

firstly observed in 321 phases. The pure phase of $\text{Nb}_3\text{As}_2\text{C}$ was obtained by an optimized synthesis process. It is found that $\text{Nb}_3\text{As}_2\text{C}$ has a bulk modulus up to 225(3) GPa as revealed by high pressure synchrotron XRD (HPXRD) study with pressure up to 47 GPa, which is confirmed by the results from the first-principles calculations. These 321 phases form a new class of the MAX family.

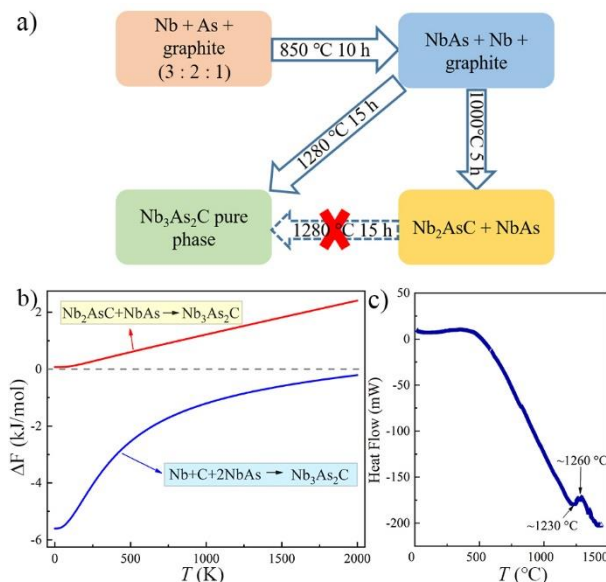


Figure 2 The synthesis of $\text{Nb}_3\text{As}_2\text{C}$ phases. (a) The synthetic process of $\text{Nb}_3\text{As}_2\text{C}$. (b) The theoretical free energy of two react paths. (c) Differential thermal analysis of 850 °C sintered sample ($\text{NbAs} + \text{Nb} + \text{C}$).

The 321 phases were synthesized by a two-step process. Take $\text{Nb}_3\text{As}_2\text{C}$ as an example, the process is illustrated in Figure 2(a). High purity Nb, As and graphite powders were mixed and sealed in an evacuated quartz tube, then heating the quartz tube to 850 °C in 20 hours, and kept for 10 hours. The main by-products are NbAs, Nb, and graphite as revealed by XRD (see Figure S1). Secondly, the as-prepared powder was pulverized, pelletized, sealed in a quartz tube, and heated to 1280 °C in 8 hours and kept for 15 hours. The end-product is $\text{Nb}_3\text{As}_2\text{C}$ with grain size 2–10 μm (Figure S2). The elemental composition determined by inductively coupled plasma-atomic emission spectrometry is Nb : As : C = 2.9 : 1.9 : 1, very close to the nominal composition. We found that long-time sintering around 1000 °C always leads to the formation of Nb_2AsC (see Figure S3), and we can not obtain 321 phase with further sintering at 1280 °C. Thermodynamic calculations (see Figure 2(b)) indicate the reaction path $\text{Nb}_2\text{AsC} + \text{NbAs} = \text{Nb}_3\text{As}_2\text{C}$ is unfavored as the free energy (ΔF) is positive. In comparison, the free energy for the reaction $\text{NbAs} + \text{Nb} + \text{C} = \text{Nb}_3\text{As}_2\text{C}$ is negative, meaning that this path is possible. The differential thermal analysis (see Figure 2(c)) confirms this. An exothermic peak at 1260 °C should be an indication of the reaction temperature, in agreement with our synthetic temperature. It is noted that $\text{Nb}_3\text{As}_2\text{C}$ will decompose under high vacuum when the sample was heated up to ~1600 °C (see Figure S4).

All peaks in the powder XRD pattern can be well indexed as $a = 3.36056(6)$ Å, and $c = 18.69508(35)$ Å with space group No. 194, $P6_3/mmc$ as shown in Figure 3(a). The crystal structure of $\text{Nb}_3\text{As}_2\text{C}$ was solved by direct method using EXPO2014 program suite^[13]. The Rietveld refinements converge to the agreement factors $R_p = 4.11\%$ and $R_{wp} = 5.45\%$. The atom positions of 321 phases are listed in Table S1. For $\text{Nb}_3\text{As}_2\text{C}$, $z_M = 0.05951(4)$, $z_A = 0.15849(5)$.

As shown in Figure 3(b), the crystal structure of $\text{Nb}_3\text{As}_2\text{C}$ exhibits distinct structural features from the conventional $\text{M}_{n+1}\text{AX}_n$ phases. There are two Nb positions in $\text{Nb}_3\text{As}_2\text{C}$ in the unit cell, as labeled by Nb1 and Nb2. Each As atoms is coordinated by three Nb1 atoms and three Nb2 atoms forming a triangular prism; Each C atom is coordinated by six Nb1 atoms forming an octahedron. Different from $\text{M}_{n+1}\text{AX}_n$ phases, the MA-triangular-prism layers here are bilayers. The crystal structure of $\text{Nb}_3\text{As}_2\text{C}$ could be seen as an alternate stacking of MX-octahedron layer and MA-triangular-prism bilayer. Similar to most MAX phases, the Nb, As, and C atoms of 321 phases are all in hexagonal closed packing positions.

The atomic arrangement in the unit cell was examined by high-angle annular dark-field (HAADF) and annular-bright-field (ABF) scanning transmission electron microscopy (STEM) as shown in Figure 3(c) and 3(d). The atomic stacking of Nb and As atoms along the [001] direction were clearly observed in HAADF and ABF images, matching well with the solved structure. Due to the low contrast of C atoms, it is hard to observe the C atoms^[14] in HAADF image. But in ABF image, C atoms can be identified lying in between the Nb atom layers. The atomically resolved HAADF and ABF images justify the reliability of the solved structure.

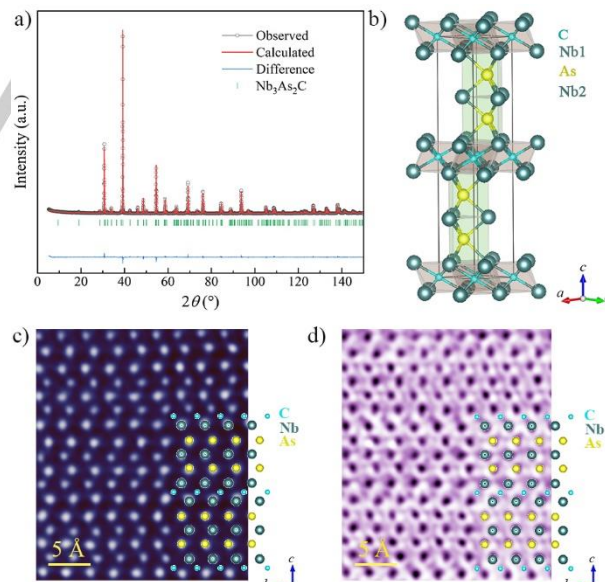


Figure 3 Crystal structure of $\text{Nb}_3\text{As}_2\text{C}$. (a) The crystal structure of $\text{Nb}_3\text{As}_2\text{C}$. (b) The Rietveld refinement of the XRD data of $\text{Nb}_3\text{As}_2\text{C}$. (c) The HAADF image of the atomic arrangement of $\text{Nb}_3\text{As}_2\text{C}$ viewed from [100] direction. (d) The ABF image.

For $\text{Nb}_3\text{As}_2\text{C}$, $d_{\text{Nb1-C}} = 2.2365$ Å is slightly shorter than the $d_{\text{Nb-C}} = 2.2422$ Å; the average of $d_{\text{Nb1-As}}$ (2.6814 Å) and $d_{\text{Nb2-As}}$ (2.5867 Å)

COMMUNICATION

is close to the $d_{\text{Nb-As}}$ (2.6343 Å) in Nb_2AsC . This suggests the strong Nb-C and Nb-As bonding in $\text{Nb}_3\text{As}_2\text{C}$ as the case in Nb_2AsC . The strong bonding strengths in this 321 phase are expected to exhibit high elastic performance as in As-, P-, S-contained 211 phases^[15].

HPXRD under pressures up to 47 GPa were applied to determine the bulk modulus of $\text{Nb}_3\text{As}_2\text{C}$. As shown in Figure 4(a), no new peak appears with the rising pressure, indicating the excellent stability of $\text{Nb}_3\text{As}_2\text{C}$ under high pressures. The strongest three peaks (105), (100), and (110) can be obviously seen to shift to high angles with increasing pressures. The pressure dependence of the normalized lattice parameters a/a_0 , c/c_0 are shown in Figure 4(b). Similar to the case with $\text{Zr}_2\text{SC}^{[15d]}$, the compressibilities of this 321 phase are quite isotropic, while are strong anisotropic^[16] for most MAX phases. Both a and c shrink by less than 6%, and the cell volume by about 16% at the pressure of 47 GPa. The pressure-dependent V/V_0 can be well fitted by the Birch–Murnaghan^[17] equation of state with a correlation coefficient $R^2 = 0.9987$,

$$P = 3 / 2 B_0 [(V / V_0)^{-7/3} - (V / V_0)^{-5/3}] \times [1 + \frac{3}{4} (B_0' - 4) (V / V_0)^{-2/3} - 1]$$

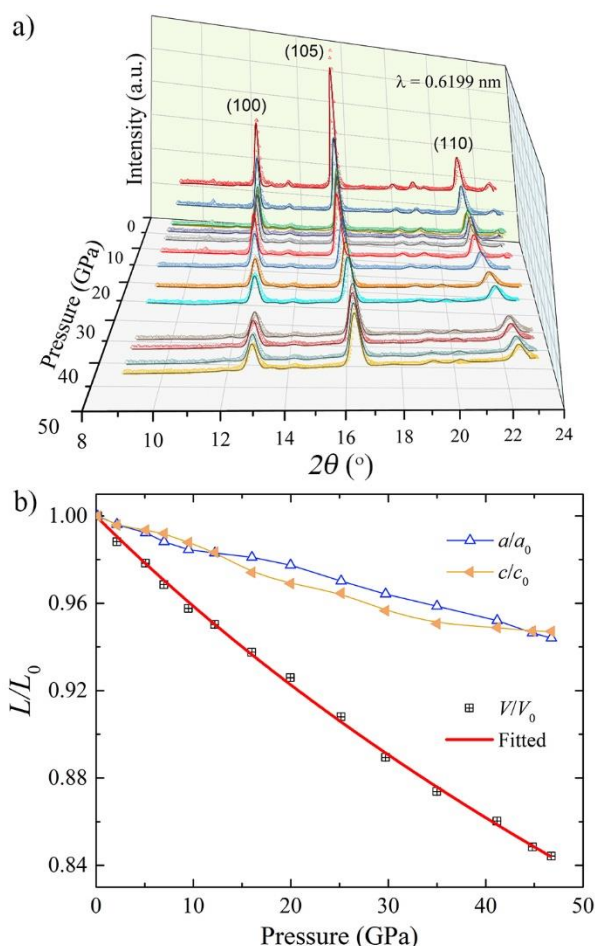


Figure 4. HPXRD study of $\text{Nb}_3\text{As}_2\text{C}$. (a) The pressure dependence of the XRD patterns of $\text{Nb}_3\text{As}_2\text{C}$, the solid lines are the results of refinements. (b) Pressure-dependent relative cell parameters (a/a_0 , c/c_0 , and V/V_0). The red curve is the fit to data by the Birch–Murnaghan equation of state.

where B_0 is the bulk modulus and B_0' its first pressure derivative. The fitted B_0 and B_0' are 225(3) GPa, and 2.6(3) GPa, respectively. The value of B_0 of $\text{Nb}_3\text{As}_2\text{C}$ is nearly equal to the $B_0 = 224(2)$ GPa for $\text{Nb}_2\text{AsC}^{[15b]}$, and quite close to the highest $B_0 = 261(2)$ GPa for $\beta\text{-Ta}_4\text{AlC}_3^{[18]}$. This result shows that the existence of more Nb-As bonds in $\text{Nb}_3\text{As}_2\text{C}$ does not cause a decrease in bulk modulus, which provide further evidence of that the M-A bonding and M-X bonding are close in strength in the As- contained MAX phases. First-principles calculations have been used to evaluate the elastic constants c_{ij} of most MAX phases within an accuracy of $\sim 10\%$ ^[19]. We performed the first-principles calculations of the elastic constants of $\text{Nb}_3\text{As}_2\text{C}$ along with other 321 phases. For hexagonal symmetry, there are five independent elastic constants: c_{11} , c_{12} , c_{13} , c_{33} , and c_{44} as shown in the Equation S1^[19]. The calculated elastic constants c_{ij} are listed in Table S2. The bulk modulus B_V , Young's modulus E_V , shear modulus G_V and Poisson ratio ν as listed in Table 1 were then calculated by the Voigt method using Equations S2–S5^[19]. The Poisson ratio ν of 321 phases are in the range of 0.22–0.24. For $\text{Nb}_3\text{As}_2\text{C}$, the bulk modulus B_V is 198.3 GPa. The calculated B_V for Nb_2AsC by the same method is near 200 GPa, consistent with the results 204 GPa calculated by Mekour et al.^[20] Accordingly, the *ab initio* calculations tend to underestimate the elastic properties of As-, P-contained MAX phases. The elastic modulus and shear modulus of $\text{Nb}_3\text{As}_2\text{C}$ ($E_V = 306.5$ GPa, $G_V = 123.4$ GPa) are slightly smaller than Nb_2AsC ($E_V = 313$ GPa, $G_V = 126$ GPa)^[21].

As shown in Table 1, the bulk modulus of $\text{Nb}_3\text{P}_2\text{C}$ and $\text{Ta}_3\text{P}_2\text{C}$ are 223.6 GPa and 222.0 GPa, respectively. Because of the underestimation of the bulk modulus in the case of $\text{Nb}_3\text{As}_2\text{C}$, the experimental bulk modulus of $\text{Nb}_3\text{P}_2\text{C}$ and $\text{Ta}_3\text{P}_2\text{C}$ might be higher than that for $\text{Nb}_3\text{As}_2\text{C}$. It can be seen that the P-contained 321 phases are better elastically performed than As-contained 321 phases. $\text{Nb}_3\text{P}_2\text{C}$ ($E_V = 371.8$ GPa, $G_V = 152.0$ GPa) performed best among 321 phases, even better than the calculated results in Nb_2PC ($E_V = 333$ GPa and $G_V = 134$ GPa)^[21]. More interestingly, the calculated results of $\text{Nb}_3\text{P}_2\text{C}$ also higher than the experimental results in Nb_4AlC_3 , which are the best values among the MAX phases ($E_V = 365$ GPa, $G_V = 149$ GPa parallel to basal plane, and $E_V = 353$ GPa, $G_V = 153$ GPa vertical to basal plane)^[22]. Considering the possible best elastic performance, relatively low theoretical density and low toxicity, $\text{Nb}_3\text{P}_2\text{C}$ is a more promising material for application among these 321 phases.

Table 1: The theoretical lattice parameters a' and c' and elastic parameters of 321 phases.

	a' (Å)	c' (Å)	G_V (GPa)	E_V (GPa)	B_V (GPa)	ν
$\text{Nb}_3\text{As}_2\text{C}$	3.3857	18.9088	123.4	306.5	198.3	0.24
$\text{Nb}_3\text{P}_2\text{C}$	3.3334	18.2091	152.0	371.8	223.6	0.22
$\text{Ta}_3\text{P}_2\text{C}$	3.3128	18.1167	149.0	365.3	222.0	0.23
$\text{V}_3\text{As}_2\text{C}$	3.1657	17.8618	121.4	297.8	181.2	0.23

Until now, the known As- or P- contained conventional MAX phases include Nb_2AsC , Nb_2PC , V_2AsC , and $\text{V}_2\text{PC}^{[7, 23]}$. The synthesis of other As- or P- contained 321 phases $\text{Ta}_3\text{P}_2\text{C}$, $\text{Nb}_3\text{P}_2\text{C}$ and $\text{V}_3\text{As}_2\text{C}$ were tried. We find these phases exist but the secondary phases MX, M_2AX or MA are often present. For

COMMUNICATION

instance, the main phase Nb₃P₂C content is 57.7(6) mol.%, and the secondary phases are NbC (5.2(1)%), Nb₂PC (22.7(2)%), NbP (14.4(2)%), see Figure S5. The Rietveld refinements were performed for Nb₃P₂C and Ta₃P₂C samples. For V₃As₂C, there are many unknown peaks in the PXRD pattern as shown in Figure S6, so we only indexed the peaks belonging to V₃As₂C to obtain its lattice parameters. The lattice parameters, atomic positions, phase content, and agreement factors of 321 phases are listed in Table S1. The structural information including the bond lengths and bond angles are listed in Table S3.

In conclusion, new series of MAX phases, Nb₃As₂C, V₃As₂C, Nb₃P₂C, and Ta₃P₂C, named as 321 phases were added to the family of MAX phases. With the optimized synthesis method, pure phase of Nb₃As₂C can be obtained, and we suggest the reaction path should follow NbAs + Nb + C = Nb₃As₂C. XRD and TEM results revealed that the 321 phases share common symmetry and constitute units with the conventional M_{n+1}AX_n phases. The structure of 321 phases consists of alternate stacking of MX-octahedron layers and MA-triangular-prism bilayers. The First-principles calculations and HPXRD reveal the outstanding elastic performance of 321 phases. The experimental bulk modulus of Nb₃As₂C is up to 225(3) GPa, which is close to the highest values among MAX phases. The predicted the elastic stiffness ($E_V = 371.8$ GPa, $G_V = 152.0$ GPa, $B_V = 223.6$ GPa), relative low density and low toxicity of Nb₃P₂C make it a most promising material for future application. These 321 phases are the first series of MAX phases that can be expressed as M_{n+1}A_nX with $n > 1$. Their novel structure and outstanding elastic stiffness in 321 phases are interesting, which is encouraging to search new M_{n+1}A_nX phases.

Acknowledgements

This work is financially supported by the National Natural Science Foundation of China under granting numbers: No. 51532010, No. 91422303; the Key Research Program of Frontier Sciences, CAS, Grant No. QYZDJ-SSW-SLH013; and the Strategic Priority Research Program of Chinese Academy of Sciences (Grant No. XDB07020100).

Keywords: MAX phase • high pressure XRD • elastic constants • layered compound • carbide

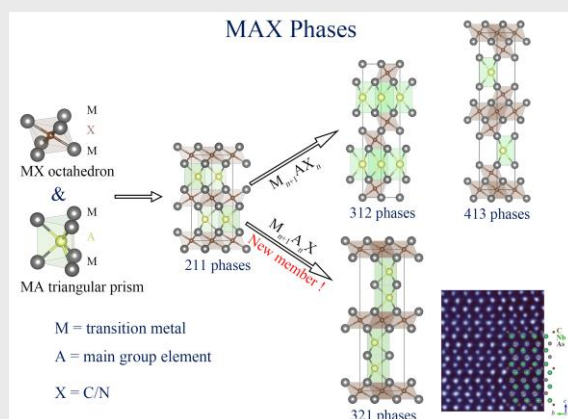
- [1] a) M. W. Barsoum, T. El-Raghy, *Am. Sci.* **2001**, *89*, 334-343; b) M. W. Barsoum, *Prog. Solid State Chem.* **2000**, *28*, 201-281; c) P. Eklund, M. Beckers, U. Jansson, H. Högborg, L. Hultman, *Thin Solid Films* **2010**, *518*, 1851-1878.
- [2] a) Z. M. Sun, *Int. Mater. Rev.* **2013**, *56*, 143-166; b) Z. M. Sun, H. Hashimoto, Z. F. Zhang, S. L. Yang, S. Tada, *Mater. Trans.* **2006**, *47*, 170-174.
- [3] M. W. Barsoum, M. Radovic, *Annual Review of Materials Research* **2011**, *41*, 195-227.
- [4] a) M. W. Barsoum, in *MAX Phases: Properties of Machinable Ternary Carbides and Nitrides*, Wiley-VCH Verlag GmbH & Co. KGaA, Weinheim, Germany, **2013**; b) M. W. Barsoum, D. Brodtkin, T. El-Raghy, *Scripta Mater.* **1997**, *36*, 535-541.
- [5] a) V. M. Hong Ng, H. Huang, K. Zhou, P. S. Lee, W. Que, J. Z. Xu, L. B. Kong, *J. Mater. Chem. A* **2017**, *5*, 3039-3068; b) M. Naguib, O. Mashtalir, J. Carle, V. Presser, J. Lu, L. Hultman, Y. Gogotsi, M. W. Barsoum, *ACS Nano* **2012**, *6*, 1322-1331; c) F. Shahzad, M. Alhabeab, C. B. Hatter, B. Anasori, S. Man Hong, C. M. Koo, Y. Gogotsi, *Science* **2016**, *353*, 1137; d) M. Ghidui, M. R. Lukatskaya, M.-Q. Zhao, Y. Gogotsi, M. W. Barsoum, *Nature* **2014**, *516*, 78; e) M. R. Lukatskaya, O. Mashtalir, C. E. Ren, Y. Dall'Agnese, P. Rozier, P. L. Taberna, M. Naguib, P. Simon, M. W. Barsoum, Y. Gogotsi, *Science* **2013**, *341*, 1502; f) M. Naguib, V. N. Mochalin, M. W. Barsoum, Y. Gogotsi, *Adv. Mater.* **2014**, *26*, 992-1005; g) O. Mashtalir, M. Naguib, V. N. Mochalin, Y. Dall'Agnese, M. Heon, M. W. Barsoum, Y. Gogotsi, *Nature Communications* **2013**, *4*, 1716.
- [6] M. Naguib, M. Kurtoglu, V. Presser, J. Lu, J. Niu, M. Heon, L. Hultman, Y. Gogotsi, M. W. Barsoum, *Advanced Materials* **2011**, *23*, 4248-4253.
- [7] O. Beekmann, H. Boller, H. Nowotny, *Monatshfte für Chemie* **1968**, *99*, 1580-1583.
- [8] a) W. Jeitschko, H. Nowotny, *Monatshfte für Chemie - Chemical Monthly* **1967**, *98*, 329-337; b) H. Wolfgruber, H. Nowotny, F. Benesovsky, *Monatshfte für Chemie und verwandte Teile anderer Wissenschaften* **1967**, *98*, 2403-2405.
- [9] M. W. Barsoum, L. Farber, I. Levin, A. Procopio, T. El-Raghy, A. Berner, *J. Am. Ceram. Soc.* **1999**, *82*, 2545-2547.
- [10] C. Hu, C. C. Lai, Q. Tao, J. Lu, J. Halim, L. Sun, J. Zhang, J. Yang, B. Anasori, J. Wang, Y. Sakka, L. Hultman, P. Eklund, J. Rosen, M. W. Barsoum, *Chem. Commun.* **2015**, *51*, 6560-6563.
- [11] O. Beckmann, H. Boller, H. Nowotny, *Monatshfte für Chemie / Chemical Monthly* **1970**, *101*, 945-955.
- [12] K. Sakamaki, H. Wada, H. Nozaki, Y. Onuki, M. Kawai, *J. Alloys Compd.* **2002**, *339*, 283-292.
- [13] A. Altomare, C. Cuocci, C. Giacomazzo, A. Moliterni, R. Rizzi, N. Corriero, A. Falcicchio, *J. Appl. Crystallogr.* **2013**, *46*, 1231-1235.
- [14] M. W. Barsoum, in *MAX Phases: Properties of Machinable Ternary Carbides and Nitrides*, Wiley-VCH Verlag GmbH & Co. KGaA, Weinheim, Germany, **2013**.
- [15] a) T. Liao, J. Wang, Y. Zhou, *J. Phys.: Condens. Matter* **2006**, *18*, L527-L533; b) R. S. Kumar, S. Rekhi, A. L. Cornelius, M. W. Barsoum, *Appl. Phys. Lett.* **2005**, *86*, 111904; c) T. Liao, J. Wang, Y. Zhou, *J. Mater. Res.* **2011**, *24*, 556-564; d) S. R. Kulkarni, N. A. Phatak, S. K. Saxena, Y. Fei, J. Hu, *J. Phys.: Condens. Matter* **2008**, *20*.
- [16] a) S. R. Kulkarni, R. S. Vennila, N. A. Phatak, S. K. Saxena, C. S. Zha, T. El-Raghy, M. W. Barsoum, W. Luo, R. Ahuja, *Journal of Alloys and Compounds* **2008**, *448*, L1-L4; b) B. Manoun, R. P. Gulve, S. K. Saxena, S. Gupta, M. W. Barsoum, C. S. Zha, *Phys. Rev. B* **2006**, *73*, 024110; c) B. Manoun, H. P. Liemann, R. P. Gulve, S. K. Saxena, A. Ganguly, M. W. Barsoum, C. S. Zha, *Applied Physics Letters* **2004**, *84*, 2799-2801.
- [17] F. Birch, *Journal of Geophysical Research: Solid Earth* **1978**, *83*, 1257-1268.
- [18] B. Manoun, S. Saxena, T. El-Raghy, M. Barsoum, *Appl. Phys. Lett.* **2006**, *88*, 201902-201902.
- [19] M. W. Barsoum, in *MAX Phases: Properties of Machinable Ternary Carbides and Nitrides*, Wiley-VCH Verlag GmbH & Co. KGaA, Weinheim, Germany, **2013**.
- [20] Y. Medkour, A. Roumili, M. Boudissa, D. Maoche, L. Louail, A. Gamoura, *Comp. Mater. Sci.* **2010**, *48*, 174-178.
- [21] M. F. Cover, O. Warschkow, M. Bilek, D. McKenzie, *J. Phys.: Condens. Matter* **2009**, *21*, 305403.
- [22] C. Hu, Y. Sakka, T. Nishimura, S. Guo, S. Grasso, H. Tanaka, **2011**, *12*, 044603.
- [23] a) H. Boller, H. Nowotny, *Monatshfte für Chemie und verwandte Teile anderer Wissenschaften* **1966**, *97*, 1053-1058; b) H. Boller, H. Nowotny, *Monatshfte für Chemie - Chemical Monthly* **1968**, *99*, 672-675.

COMMUNICATION

Entry for the Table of Contents (Please choose one layout)

Layout 2:

COMMUNICATION



Hongxiang Chen, Dongliang Yang,
Qinghua Zhang, Shifeng Jin, Liwei Guo,
Xiaodong Li, Xiaolong Chen*

Page No. – Page No.
New series of MAX phases with MA-triangular-prism bilayers: synthesis, structure, and elastic properties

New series of MAX phases with outstanding elastic properties, named as 321 phases, were added to MAX phases family. 321 phases share common symmetry and constitute units with the conventional $M_{n+1}A_nX_n$ phases. Different from $M_{n+1}A_nX_n$ phases, the MA-triangular-prism layers here are combined into bilayers. 321 phases are the first series of MAX phases that can be expressed as $M_{n+1}A_nX$ with $n > 1$.